Assessing Groundwater Model Uncertainty for the Central Nevada Test Area

Greg Pohll[1], Karl Pohlmann[2], Ahmed Hassan[2], Jenny Chapman[2], and Todd Mihevc[1]
[1]*Desert Research Institute, Division of Hydrologic Sciences, 2215 Raggio Parkway, Reno, NV 89512*
[2]*Desert Research Institute, Division of Hydrologic Sciences, 755 E. Flamingo Road, Las Vegas, NV 89119*

Abstract - *The purpose of this study is to quantify the flow and transport model uncertainty for the Central Nevada Test Area (CNTA). Six parameters were identified as uncertain, including the specified head boundary conditions used in the flow model, the spatial distribution of the underlying welded tuff unit, effective porosity, sorption coefficients, matrix diffusion coefficient, and the geochemical release function, which describes nuclear glass dissolution. The parameter uncertainty was described by assigning prior statistical distributions for each of these parameters. Standard Monte Carlo techniques were used to sample from the parameter distributions to determine the full prediction uncertainty. Additional analysis is performed to determine the most cost-beneficial characterization activities. The maximum radius of the tritium and strontium-90 contaminant boundary was used as the output metric for evaluation of prediction uncertainty. The results indicate that combining all of the uncertainty in the parameters listed above propagates to a prediction uncertainty in the maximum radius of the contaminant boundary of 234 to 308 m and 234 to 302 m, for tritium and strontium-90, respectively. Although the uncertainty in the input parameters is large, the prediction uncertainty in the contaminant boundary is relatively small. The relatively small prediction uncertainty is primarily due to the small transport velocities such that large changes in the uncertain input parameters cause small changes in the contaminant boundary. This suggests that the model is suitable in terms of predictive capability for the contaminant boundary delineation.*

I. INTRODUCTION

The Central Nevada Test Area (CNTA) is located about 95 km northeast of Tonopah and 175 km southwest of Ely, Nevada (Figure 1).[1] The only underground nuclear test conducted at CNTA was Faultless. The Faultless test consisted of a 200- to 1,000-kt-yield nuclear detonation, which occurred on January 19, 1968.[2] Faultless was designed to study the behavior of seismic waves generated by a nuclear test in Hot Creek Valley and evaluate the usefulness of the site for higher-yield tests.

The Desert Research Institute (DRI) has been tasked by the U.S. Department of Energy (DOE) to characterize the subsurface hydrogeologic environment and to construct a groundwater flow and transport model. The purpose of the model is to formalize the conceptual model of the flow and transport system, predict future migration of test-related solutes, and quantify the uncertainty in the model predictions.

A groundwater flow and transport model was used to determine the potential radionuclide transport due to the Faultless nuclear detonation.[3] A certain degree of uncertainty exists in the ability of this model to predict solute migration. This output uncertainty is due to uncertainty in the conceptual model, input parameters and the ability of the mathematical model to effectively simulate real-world conditions. A data decision analysis (DDA) uses the groundwater model in conjunction with known input parameter uncertainties to determine the overall prediction uncertainty. Potential characterization activities are assessed based on each activity's ability to reduce prediction uncertainty at a reasonable cost. The prediction uncertainty is then assessed to determine if the predictive capability of the model is acceptable. If the model is deemed acceptable, then contaminant boundary predictions are made, and if not, potential characterization activities are assessed in terms of their ability to reduce model uncertainty through a cost-benefit analysis.

II. METHODOLOGY

Uncertain Parameters

The first step required in the DDA is to identify the uncertain model parameters. These parameters were identified based on the sensitivity analysis performed during the modeling phase.[3] Of the many parameters required to construct the numerical model, six were

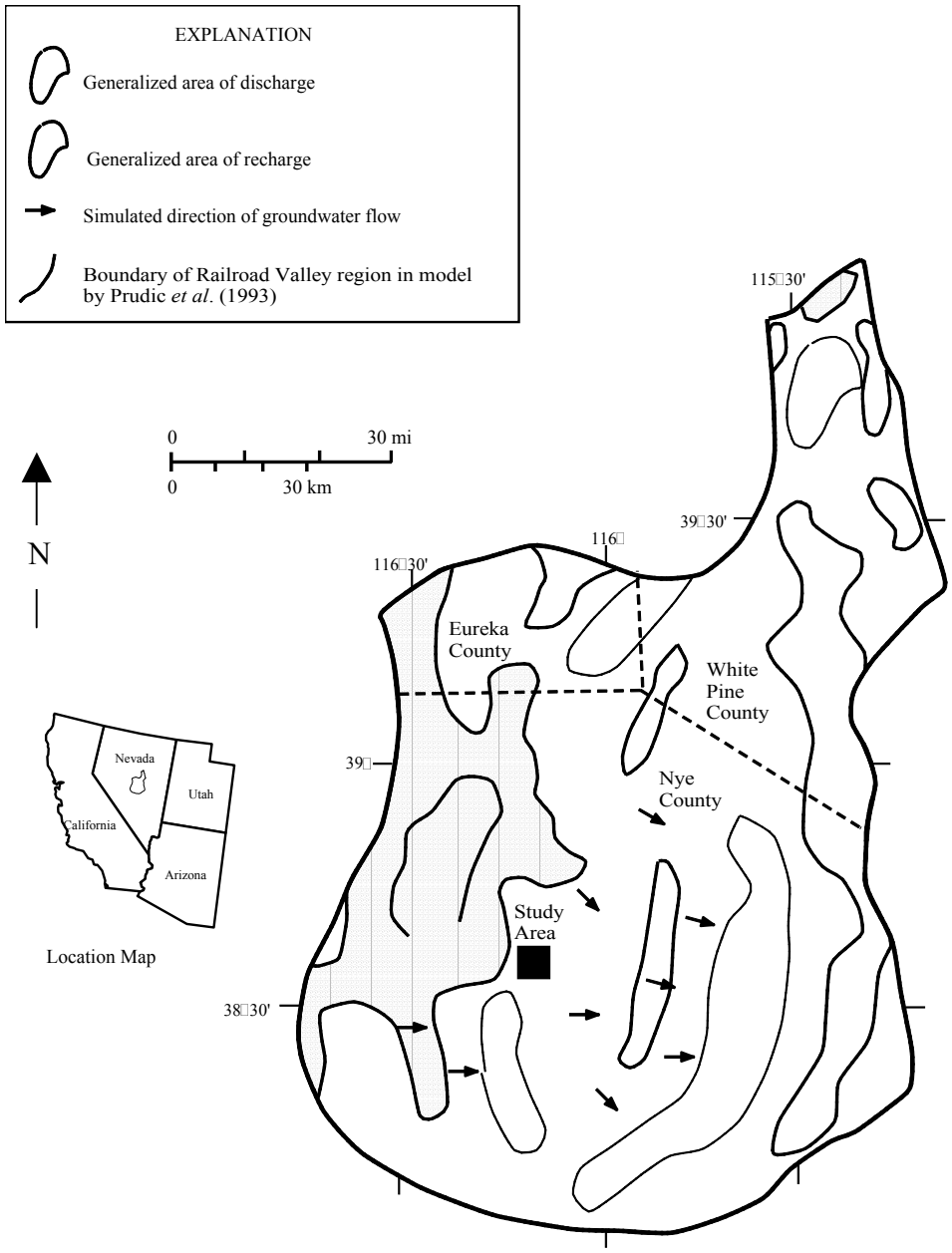

Figure 1. Simplified view of the Railroad Valley region with regional groundwater flow directions.

identified as uncertain in terms of the model's ability to predict solute migration. These parameters include:

1. Specified head boundary conditions.
2. The spatial distribution of the underlying welded tuff unit.
3. Effective porosity.
4. Sorption coefficients.
5. Matrix diffusion coefficient.
6. Geochemical release function (nuclear glass dissolution).

There are other parameters that are uncertain, but these were found to be the most important in terms of predicting solute migration. It is also important to note that although hydraulic conductivity is not listed as an uncertain parameter, uncertainty in this parameter is included in the model through a stochastic treatment of a spatially heterogeneous distribution of hydraulic conductivity.

Prior Distributions

The first step in any type of uncertainty analysis is to assess the range of potential values that an individual parameter can take, and the associated probability associated with a given value. A common method of defining these ranges and associated probabilities is through the use of a probability distribution function (PDF). There are various analytic expressions that statisticians use to quantify a PDF, some of which include uniform, normal, and log-normal.

A PDF that describes the current state of knowledge about an individual parameter is known as a prior distribution. A prior distribution represents the degree of belief about the parameter prior to collection of additional data. Parameter uncertainty is first described by a functional PDF (*e.g.,* normal, log-normal, uniform, uniform $\log_{10}$) and then by its assumed mean and variance.

The type of distribution chosen to represent the uncertainty is based on how the assessment was undertaken. For example, if site-specific data were available, then a fitting program was used to determine the most appropriate distribution that represents the data. If data were not available, and literature values were used, then a uniform distribution was assumed. If the range spanned many orders of magnitude, then a uniform $\log_{10}$ distribution was used to properly simulate the large range in uncertainty. In some cases, the form of the distribution was determined based on regression error analysis and/or spatial statistics, in which case the distribution form is determined directly from the analysis.

The uncertainty associated with the specified head boundary conditions was determined via an error analysis associated with the horizontal and vertical gradients. The specified head boundary conditions applied along the northern, southern and lowermost boundaries were constant. A linear regression was performed using the hydraulic heads at HTH-1, which is located near the center of the model domain, and for which vertical head

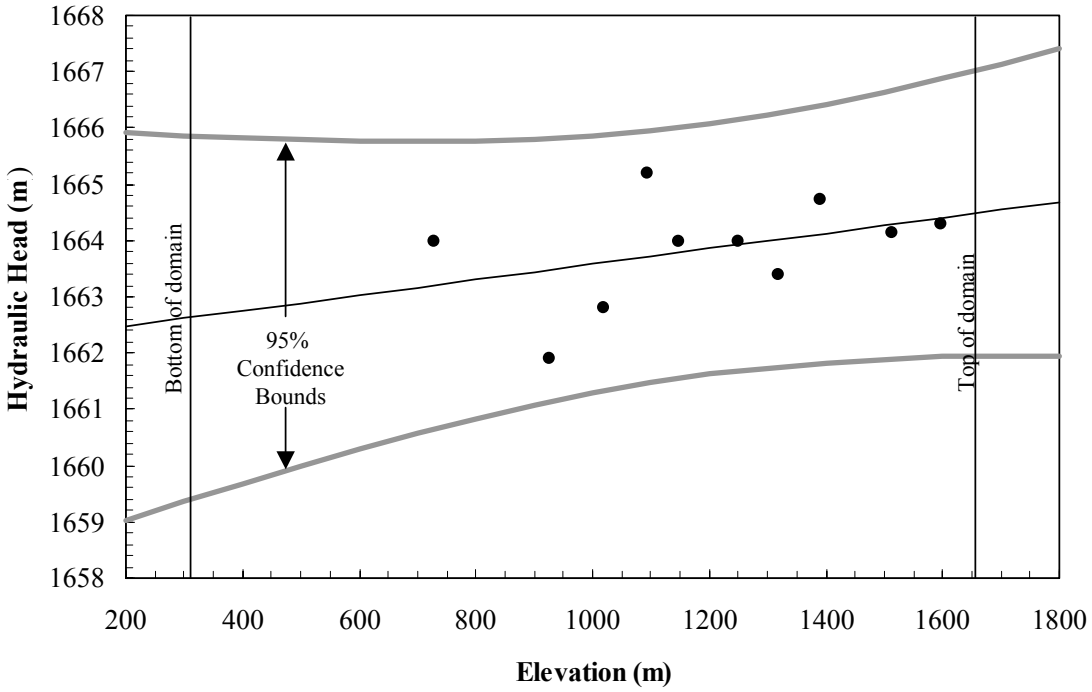

Figure 2. Vertical hydraulic head measurements and associated prediction uncertainty.

All available data were used to assess the current state of uncertainty for each of the uncertain parameters. If site-specific data were not available, then literature values were used to specify a range of possible values.

gradients were available. Figure 2 shows the linear regression line and the associated 95 percent confidence intervals associated with the fit. The error associated with the regression line is normally distributed with the mean equal to the regression line and the standard deviation

being defined by the regression error. The regression line and its associated error were used to randomly sample for the hydraulic head at the top and bottom of the model domain at the northing position determined by HTH-1.

A similar process was performed to determine the uncertainty in the hydraulic head gradient at the top and bottom of the model domain, using data obtained at UCE-20, HTH-1, and UCE-18. The horizontal gradient was randomly sampled at the top and bottom of the model domain according to the regression analysis. The gradient and the hydraulic head from the previous sampling (at the HTH-1 northing position) were used to extrapolate the head along the upper and lower boundaries. The two vertical boundary heads were calculated via a simple linear interpolation.

The simulation of the three hydrogeologic categories were generated using a sequential indicator approach.[4] The previous groundwater flow and transport model was three-dimensional and this DDA used a two-dimensional model domain so three-dimensional fields were generated to preserve the spatial statistics, but only the center section (along the north-south direction) was used for the DDA model. The uncertainty in the location of the welded tuff is unique for each realization, except at nodes where conditioning data are available. Realizations where the welded tuff is simulated as being near the test location have a much larger probability of fast transport as the mean hydraulic conductivity of the welded tuff is two- and three-orders of magnitude larger than the alluvium and tuffaceous sediments, respectively. Although hydraulic conductivity is not explicitly stated as an uncertain parameter, the simulation of geologic heterogeneity is being simulated, which translates into spatial variability in hydraulic conductivity as each hydrogeologic unit has a unique conductivity. Therefore, for each Monte Carlo realization, a unique pattern of hydraulic conductivity is created.

The uncertainty in the effective porosity is determined through a combination of literature values and site-specific data. Total porosity estimates were determined for cores within the welded tuff, tuffaceous sediments and alluvium. Although total porosity estimates determined within the laboratory measure only the void space within the pores, it was assumed that this was a good approximation of effective porosity for the alluvium and tuffaceous sediments. Lognormal distributions were used to describe the uncertainty for these units. A uniform $\log_{10}$ distribution was used to describe the effective porosity for the welded tuff unit with the range being determined from literature values. It was assumed that flow and transport within the welded tuff was dominated by fracture flow and as such effective porosities need to describe the void space due to the fractures and not the matrix. Table 1 lists parameters used to define each of the three distributions.

The sorption process was simulated using a linear isotherm, which is described via a retardation coefficient within the transport model. Of the two solutes analyzed within the DDA, strontium-90 is the only one that sorbs. Laboratory batch experiments were performed to determine the retardation coefficients for strontium-90 for

Table 1. Parameters used to describe the uncertainty in effective porosity for the three hydrogeologic units.

Parameter	Units	Distribution Type	Source	Mean	Standard Deviation
Effective Porosity (Alluvium)	m^3/m^3	Lognormal	CNTA Database	2.92	0.30
Effective Porosity (Welded Tuff)	m^3/m^3	Uniform Log_{10}	Literature	-2.50	0.08
Effective Porosity (Tuffaceous Sediments)	m^3/m^3	Lognormal	CNTA Database	2.78	0.42

Note: Mean and standard deviation are presented in natural log space for lognormal distributions and $\log_{10}$ space for uniform $\log_{10}$ distributions

each of the three hydrogeologic units.[5] The retardation term for alluvium and tuffaceous sediments is calculated as:

$$R = 1 + \frac{\rho b K_d}{\theta} \qquad (1)$$

where ρ_b is the bulk density (g/cm^3), K_d is the distribution coefficient determined as a ratio of the mass of sorbate sorbed per sorbed mass of sorbent to the aqueous concentration of sorbate (cm^3/g), and θ (cm^3/cm^3) is the porosity. Fracture flow systems (*e.g.* welded tuff) typically require a modification to the retardation calculation as:

$$R = 1 + \frac{2K_a}{b} \qquad (2)$$

where K_a (cm) is the surface-based sorption constant ($K_a = K_d/A_{sp}$), b is the fracture aperture (cm), and A_{sp} is the specific surface area of the sorbent (cm^2/g).

The K_d values are determined via linear regression of the equilibrium concentration versus sorbed concentration, with the slope being the K_d. Uncertainty in the K_d estimates is performed by standard linear regression error analysis. The K_d is only one component of the retardation term, so the stochastic terms (K_d, porosity or fracture aperture) are sampled from their respective distributions and then the retardation term is calculated using either equation (1) or (2). Table 2 lists the parameters used to define the uncertainty for the four retardation terms (alluvium, tuffaceous sediments, welded tuff - fracture, welded tuff - matrix).

Matrix diffusion is a potentially important mass transfer process by which solutes are removed from high-velocity fracture flowpaths into the surrounding matrix. Matrix diffusion is only defined for the welded tuff units, as it is assumed that matrix diffusion does not occur in the alluvium and tuffaceous sediments. The matrix diffusion parameter is defined as:[4]

$$\kappa = \frac{\theta_m \sqrt{D_m^* R_m}}{b} \qquad (3)$$

where θ_m is the matrix porosity (cm^3/cm^3), D_m^* is the effective diffusion coefficient in the rock matrix (cm^2/day), R_m is the dimensionless retardation coefficient in the rock matrix, and b is the fracture half aperture (cm). All of the parameters in equation (3) are assumed to be random, so the distribution of κ is determined by sampling from each of the parameter distributions and then calculating κ. The retardation term is assumed to be unity except when simulating strontium-90. Table 3 lists the parameters used to define the uncertainty in the matrix diffusion parameter.

Table 2. Parameters used to describe the uncertainty in the retardation coefficient for the three hydrogeologic units.

Parameter	Unit	Distribution Type	Currently Available Data	Mean	Standard Deviation
Effective Porosity (Alluvium)	m^3/m^3	Lognormal	CNTA Database	2.92	0.30
Effective Porosity (Welded Tuff)	m^3/m^3	Uniform Log10	Literature	-2.50	0.08
Effective Porosity (Tuffaceous Sediments)	m^3/m^3	Lognormal	CNTA Database	2.78	0.42
Kd - Alluvium	m^3/g	t_1 distribution	Laboratory experiments	1.32E-02	1.30E-03
Kd - Tuffaceous Sediments	m^3/g	t_1 distribution	Laboratory experiments	1.16E-03	1.14E-04
Kd - Welded Tuff - Kd (Matrix)	m^3/g	t_1 distribution	Laboratory experiments	6.11E-04	2.22E-05
Ka - Welded Tuff - (Fracture)	(m)	t_1 distribution	Laboratory experiments	9.79E-05	3.56E-06
Fracture Half-aperture	m	Uniform Log10	Literature	1.00E-04	0.58

All distribution coefficients are in the space as defined by the distribution (i.e., lognormal in natural log space, uniform $\log_{10}$ are in log10 space, etc.)
All sorption and retardation parameters refer to strontium

Table 3. Parameters used to describe the uncertainty in the matrix diffusion parameter for the welded tuff unit.

Parameter	Unit	Distribution Type	Currently Available Data	Mean	Standard Deviation
Retardation - Welded Tuff (Matrix)	(dimensionless)	numerical	Laboratory experiments	----	----
Effective Diffusion Coef.	m^2/day	Uniform $\log_{10}$	Literature	-5.91E+00	0.087
Fracture Half-aperture	m	Uniform $\log_{10}$	Literature	1.00E-04	0.58
Matrix Porosity (Welded Tuff)	m^3/m^3	lognormal	CNTA Database	2.68	0.39

All distribution coefficients are in the space as defined by the distribution (i.e., lognormal in natural log space, uniform $\log_{10}$ are in log10 space, etc.)
All sorption and retardation parameters refer to strontium

The rock, fission products, and device components that are vaporized by the tremendous heat and pressure of a nuclear reaction quickly begin to condense and coalesce into nuclear melt glass. This glass contains much of the radioactivity produced by a nuclear test and radionuclides must be removed from the melt glass to be transported by groundwater. The dissolution of the glass can be described by :

$$M_r = M_g \exp\left(-k_g t\right) \qquad (4)$$

where M_r is the amount of solute released at time t (g), M_g is the total mass of glass, k_g is the geochemical release rate (1/day), which can be calculated as:

where k_l is the linear rate constant used to describe the linear mass transfer from the solid to the liquid phase

$$k_g = k_l A_{sp} G_{fw} \qquad (5)$$

(moles/cm^2), A_{sp} is the specific surface area of the glass matrix (cm^2/g), and G_{fw} is the gram formula weight of the glass matrix (g/mole). The prior distributions for kg are determined by randomly sampling from the distribution for specific surface area and then calculating kg using equation (5). A uniform $\log_{10}$ distribution (μ=1.5, σ=.08) was used to describe the uncertainty for the specific surface area.

III. FLOW AND TRANSPORT MODEL

The three-dimensional model was converted to a two-dimensional model for use in the DDA. Figure 3 shows the two-dimensional representation used in the modeling process. A vertical cross section aligned north-south was selected as one that represents the centermost x position within the three-dimensional model. This process of converting a three-dimensional model to a two-dimensional model was straightforward, as the boundary conditions in the three-dimensional model were constant along the x-direction (east-west).

All parameters not listed above as being stochastically represented are deterministic and identical to the previous model. The only exception is the time step lengths (dt). The time steps were altered to preserve courant numbers less than one, given the revised velocity fields. This ensures that particles in the transport model do not move a distance greater than one grid cell (50 m) in any one time step. Two solutes were used for the transport modeling to assess the transport features for a conservative (tritium) and reactive (strontium-90) solute. The transport was simulated over a period of 1,000 years over which time the contaminant boundary was calculated. The initial mass is the mass as presented in unclassified documents. A contaminant boundary is calculated such that it represents an area whereby the simulated concentration exceeded the maximum contaminant level as defined by the U.S. Environmental Protection Agency (EPA) at any time during the 1,000-year simulation. The maximum radius was then calculated by measuring the distance between the center of the test area and the center of the cell furthest away. The maximum radius was used to determine the uncertainty in the predictive capability of the model and how this uncertainty would be reduced if other characterization activities were employed.

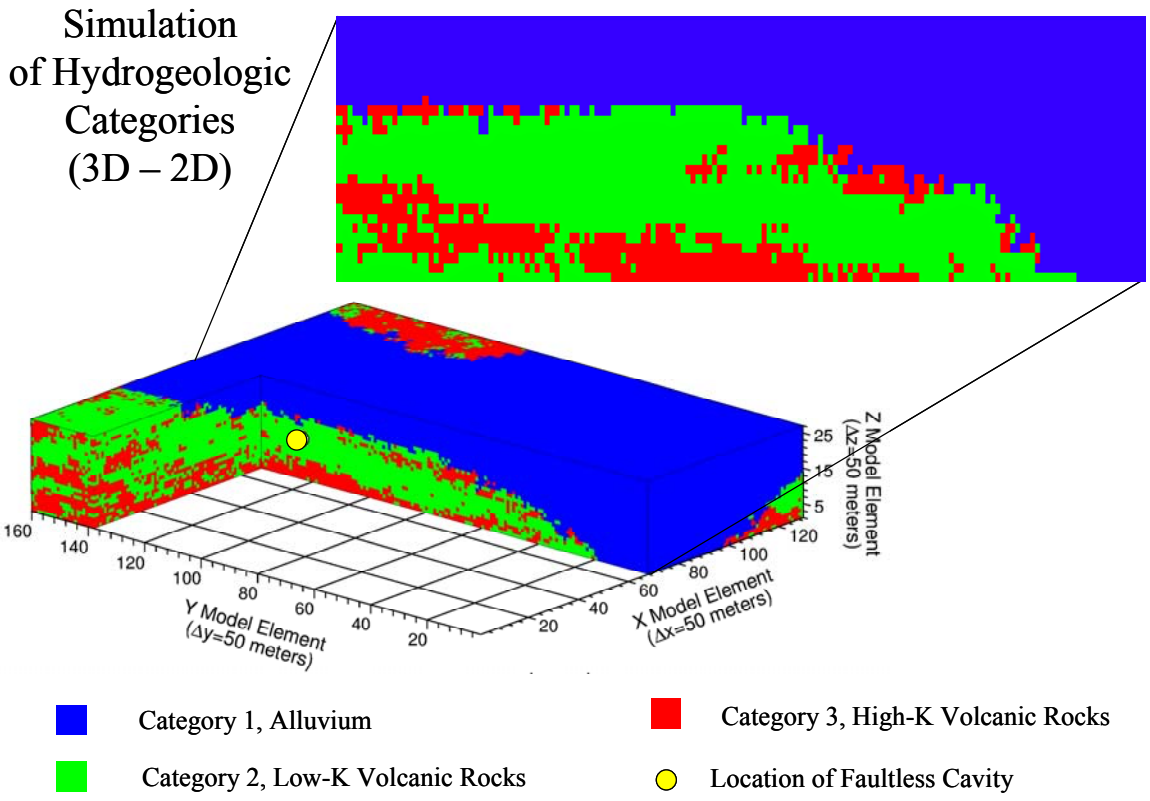

Figure 3. Model conversion from three-dimensional to two-dimensional domain. The spatial distribution of lithologic categories is one of the many equiprobable realizations.

IV. COST-BENEFIT ANALYSIS

In an effort to determine the efficacy of the potential characterization activities, a cost-benefit analysis was performed. Eleven potential characterization activities were chosen such to reduce the uncertainty in the six uncertain input parameters. An expert panel is used to provide a subjective assessment of the ability of an activity to reduce input parameter uncertainty. This information is used in a Bayesian analysis to calculate the posterior distributions for each input parameter assuming an activity was performed. The posterior distributions are then used in a Monte Carlo analysis to determine the reduction in prediction uncertainty for a given characterization activity. The cost-benefit analysis is performed by plotting the uncertainty reduction versus cost to determine the activities that provide the largest uncertainty reduction per unit cost.

Characterization Activities and Costs

Eleven characterization activities were identified to potentially reduce the uncertainty in the identified uncertain parameters. These activities include:

1. Hydrogeologic characterization well: The purpose of this activity is to obtain information on vertical hydraulic head and lithology to a depth of 1,300 m.

2. Tracer test - alluvium: The purpose of this activity is to perform a forced-gradient dipole tracer test to determine the effective porosity and other transport properties within the alluvium.

3. Tracer test - welded tuff: The purpose of this activity is to perform a forced-gradient dipole tracer test to determine the effective porosity and other transport properties within the welded tuff.

4. Tracer test tuffaceous sediment: The purpose of this activity is to perform a forced-gradient dipole tracer test to determine the effective porosity and other transport properties within the tuffaceous sediments.

5. Barometric test - alluvium: The purpose of this activity is to measure water level changes and barometric pressure in a well completed within

the alluvium (*e.g.*, HTH-1) such that an estimate of the effective porosity within the alluvium can be made.

6. Cavity drillback: Core samples within the test cavity would be collected to evaluate glass composition and dissolution, and search for reaction products that may mantle surfaces. Groundwater samples would reveal the dissolved component coexisting with the solid phase.

7. Matrix diffusion analogues: An extensive literature review would be performed to determine the most appropriate value and expected range for the matrix diffusion coefficient for a welded tuff unit.

8. Core studies for matrix diffusion: Additional laboratory experiments on welded tuff would be performed to determine the most appropriate value and expected range for the matrix diffusion coefficient for a welded tuff unit.

9. Yucca Mountain analogues for retardation: An extensive literature review would be performed to determine the retardation coefficients for the three hydrogeologic units.

10. Bullion test analogues for effective porosity: Additional research to ascertain the most appropriate value for the effective porosity for the three hydrogeologic units.

11. Additional sorption laboratory experiments: Additional laboratory batch experiments to determine the most appropriate value for the sorption/retardation coefficients for the three hydrogeologic units.

The estimated costs associated with each activity are provided in Table 4.

Expert Panel

An expert panel was organized to provide input on how well a field activity may reduce the uncertainty in the input parameters. To simplify the procedure the expert panel was asked to provide a reliability factor for each parameter that is impacted by a particular field activity. The reliability factor is a number between 0 and 1 such that a value of one would indicate the field activity provides complete uncertainty reduction, while a value of zero would imply no information gain.

The individual factors where tallied from the panel and then were averaged to eliminate bias. The averaged results are provided in Table 5. These reliability factors are then used to calculate the posterior distributions.

Table 4. Estimated costs for the proposed charactization activities

#	**Characterization Activity**	**Total Cost**
1	Hydrogeologic characterization well	$3,550,300
2	Tracer test - alluvium	$1,692,167
3	Tracer test - welded tuff	$1,992,906
4	Tracer test - tuff sediments	$2,488,231
5	Barometric test in alluvium	$57,953
6	Post-test hole for glass sample	$2,165,780
7	Matrix diffusion analogues?	$10,000
8	Core studies for matrix diffusion?	$50,000
9	Yucca Mtn. analogues for retardation?	$10,000
10	Bullion test analogues for effective porosity?	$10,000
11	Additional sorption laboratory experiments	$144,000

Table 5. Average reliability coefficients as determined by the expert panel.

Characterization Activity	Effective Porosity (Alluvium)	Effective Porosity (Welded Tuff)	Effective Porosity (Tuffaceous Sediments)	Retardation	Effective Diffusion Coef.	Fracture Half-aperture	Matrix Porosity (Welded Tuff)	Matrix Retardation	Linear Dissolution Rate Const.	Specific Surface Area
Hydrogeologic characterization well	0.00	0.00	0.00	0.00	0.00	0.37	0.00	0.00	0.00	0.00
Tracer test - alluvium	0.73	0.00	0.00	0.63	0.00	0.00	0.00	0.00	0.00	0.00
Tracer test - welded tuff	0.00	0.72	0.00	0.53	0.77	0.57	0.60	0.53	0.00	0.00
Tracer test - tuff sediments	0.00	0.00	0.73	0.63	0.00	0.00	0.00	0.00	0.00	0.00
Barometric test in alluvium	0.70	0.00	0.00	0.00	0.00	0.00	0.00	0.00	0.00	0.00
Post-test hole for glass sample	0.00	0.00	0.00	0.00	0.00	0.00	0.00	0.00	0.67	0.63
Matrix diffusion analogues	0.00	0.00	0.00	0.00	0.57	0.47	0.50	0.50	0.00	0.00
Core studies for matrix diffusion	0.00	0.00	0.00	0.00	0.70	0.00	0.73	0.73	0.00	0.00
Yucca Mtn. analogues for retardation	0.00	0.00	0.00	0.53	0.00	0.00	0.00	0.57	0.00	0.00
Bullion test analogues for effective porosity	0.00	0.57	0.20	0.00	0.00	0.00	0.00	0.00	0.00	0.00
Additional sorption laboratory experiments	0.00	0.00	0.00	0.77	0.00	0.00	0.67	0.00	0.00	0.00

Posterior Distributions

The reliability coefficients are used to calculate the posterior distributions by a simple transformation of the standard deviation:

$$\sigma_{post} = \sigma\, prior(1-\lambda) \qquad (6)$$

where σ_{post} is the posterior distribution standard deviation, σ_{prior} is the prior distribution standard deviation, and λ is the reliability coefficient. The type (i.e., normal, uniform, etc.) and the mean of the posterior distribution are assumed to be identical to the prior distribution. This assumption implies that the field activities will not produce a significantly different mean than is specified by the prior distributions. Equation (6) was used to derive the posterior distributions for all of the parameters except the constant head boundary condition and distribution of the welded tuff. The posterior distributions were derived by sampling the hydraulic head and lithologic distribution from a hypothetical well. The hypothetical well is located at a northing position of 430000 m and was sampled over the entire vertical section of the domain. The hydraulic head information gained from the hypothetical well was used to constrain the upper- and lowermost head values such that the uncertainty in the boundary conditions was then dominated by the horizontal gradients and not the vertical gradients previously determined from HTH-1. The lithologic information was used to further condition the simulation of the hydrogeologic categories via sequential indicator simulation.

Hydraulic head values were also used to weight the Monte Carlo realizations such that models with head values that were in better agreement with the sampled head values were given more weight. The methodology to properly weight the stochastic simulations has

predominantly been used in rainfall-runoff modeling but is easily extended to groundwater models.[6-7] The sampling procedure is based on a combination of Bayesian and Monte Carlo techniques. A large number of Monte Carlo model runs are made, each parameterized with random values selected from posterior distributions described above for each field activity. In the case of the hydrogeologic characterization well activity, the simulated hydraulic heads are compared to heads sampled from the hypothetical well. A likelihood measure is used to compare the effectiveness of a particular realization to represent the sampled head values as:

$$L\left(Y\middle|\theta_i\right)=\left(\sigma_i^2\right)^{-N} \qquad (7)$$

where $L(Y \mid \theta_i)$ is the likelihood of the simulated the head values Y given the parameter set θ_i for realization i, σ_i^2 is the variance of the errors, and N is a shaping factor, which was set to a value of two in this numerical experiment. The likelihood equation is then combined with Bayes equation in the form:

where $L_0(\theta_i)$ is the likelihood measure for each parameter set, which is defined by the posterior distributions for each characterization activity, $L(\theta_i|Y)$ is the posterior

$$L\left(\theta_i\middle|Y\right)=\frac{L\left(Y\middle|\theta_i\right)L_0\left(\theta_i\right)}{C} \qquad (8)$$

likelihood for the simulation of Y given θ_i, and C is a scaling constant such that the weights sum to one.

The ability of each characterization activity to reduce prediction uncertainty is tested by performing the Monte Carlo analysis with the posterior distributions defined for each activity. In the case of activity 1, the Bayesian Monte Carlo analysis was used. The reduction in parameter uncertainty is calculated as:

$$\Phi_i = 1-\frac{\Delta_{90}^{activity_i}}{\Delta_{90}^{base}} \qquad (9)$$

where Φ_i is the reduction in relative model uncertainty between the total input uncertainty case and the case where input parameter uncertainty is reduced due to a single characterization activity i, $\Delta_{90}{}^{activity}{}_i$ is the 90 percent confidence range in maximum contaminant radius calculated for an individual activity, and $\Delta_{90}{}^{base}{}_i$ is the 90 percent confidence range in maximum contaminant radius calculated for the total uncertainty case.

V. RESULTS

The total uncertainty in the contaminant boundary radius for tritium and strontium-90 is presented in Figures 4 and 5, respectively. The 90 percent confidence interval for maximum contaminant boundary stabilized after approximately 200 realizations and for the base model ranged between 234 to 308 m and 234 to 302 m, for tritium and strontium-90, respectively. The range between the upper and lower 90 percent confidence intervals was used as an uncertainty measure for comparison with the other simulations. The uncertainty range is 74 and 68 m for tritium and strontium-90, respectively.

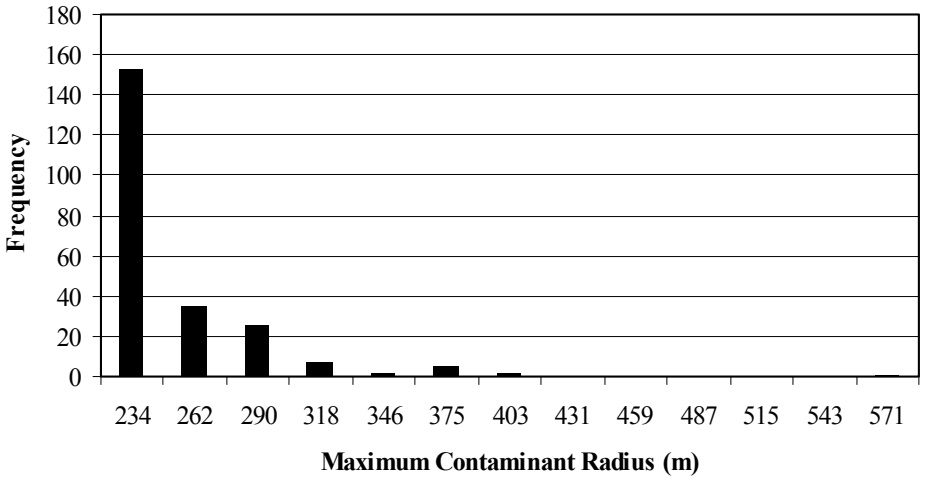

Figure 4. Histogram of maximum contaminant distance for tritium.

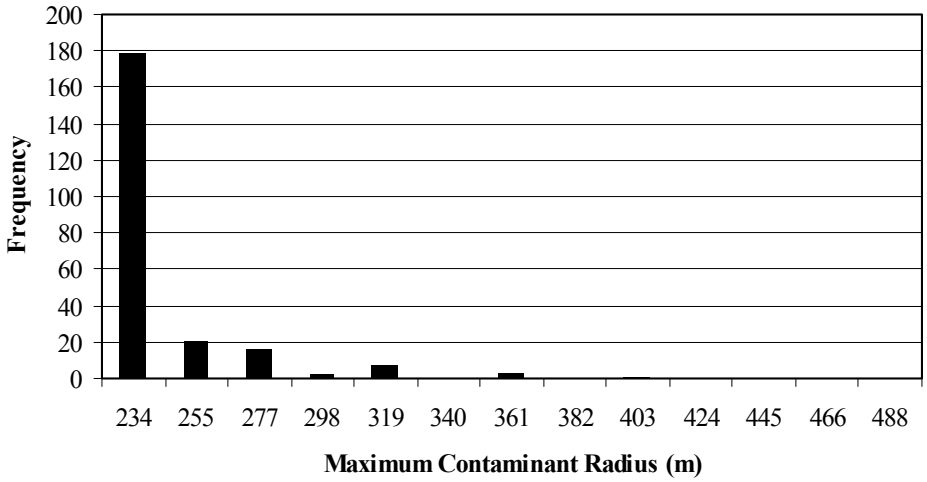

Figure 5. Histogram of maximum contaminant distance for strontium-90.

These results indicate that although there is a large amount of uncertainty in the input parameters, the uncertainty in the prediction of the contaminant boundary, within a 1,000-year time period, is relatively certain, with the error being less than 100 m. The relatively high degree of prediction certainty is primarily due to the low transport velocities. Solutes are not migrating large distances within the 1,000-year time period that defines the contaminant boundary. As such, relatively large changes in the input parameters cause small changes in the contaminant boundary. The only exception to this is in the rare event that welded tuff is simulated as being near the working point with a very small effective porosity.

The relatively small prediction uncertainty suggests that the model is suitable in terms of predictive capability for contaminant boundary delineation. As expected, these activities will further reduce the uncertainties, but reducing the current error in the uncertainty range in the contaminant boundary radius to values less than 74 and 68 m for tritium and strontium-90, respectively, may provide little value regarding management of the site.

The simulated range in the 90 percent confidence bounds and relative uncertainty reduction estimates are provided in Table 6 for tritium and strontium-90. The

Table 6. Simulated range in the 90 percent confidence bounds and relative uncertainty reduction for tritium and strontium-90.

Number	Activity	Tritium Range	Sr-90 Range	Unc. Red Tritium (%)	Unc. Red Sr-90 (%)
Base	---	74	68	---	---
1	Hydrogeologic characterization well	6	5	91.9	92.6
2	Tracer test - alluvium	67	48	9.5	29.4
3	Tracer test - welded tuff	74	48	0.0	29.4
4	Tracer test - tuffaceous sediments	74	47	0.0	30.9
5	Barometric test in alluvium	41	35	44.6	48.5
6	Post-shot hole for glass sample	48	35	35.1	48.5
7	Matrix diffusion analogues	48	35	35.1	48.5
8	Core studies for matrix diffusion	68	48	0.0	29.4
9	Yucca Mtn. analogues for retardation	68	48	0.0	29.4
10	Bullion test analogues for effective porosity	73	35	1.4	48.5
11	Laboratory sorption experiments	72	41	0.0	39.7

results clearly indicate that the hydrogeologic characterization well significantly decreases the uncertainty in the prediction of the contaminant boundary. The hydrogeologic characterization well is also the most expensive task, so it is important to understand the relative value given that the uncertainty is already small.

To ascertain the relative cost-benefit of additional characterization activities, one can plot the cost versus uncertainty reduction. These plots are provided in Figures 6 and 7 for tritium and strontium-90, respectively. Those activities that plot in the upper left-hand corner can be considered the optimal activities in terms of cost versus benefit as they have the largest uncertainty reduction per unit cost. The optimal activities include the barometric test, matrix diffusion analogues, and the hydrogeologic characterization well for both tritium and strontium-90 contaminant boundaries. The Bullion test analogues for effective porosity proved to be optimal, but only for the strontium-90 contaminant boundary. The activities that were not found to be optimal were either too expensive or simply not important in terms of predicting the contaminant boundary.

Although the optimal activities represent the greatest uncertainty reduction per unit cost, the current level of uncertainty for the contaminant boundary is small and may be deemed acceptable, thereby not requiring improvement.

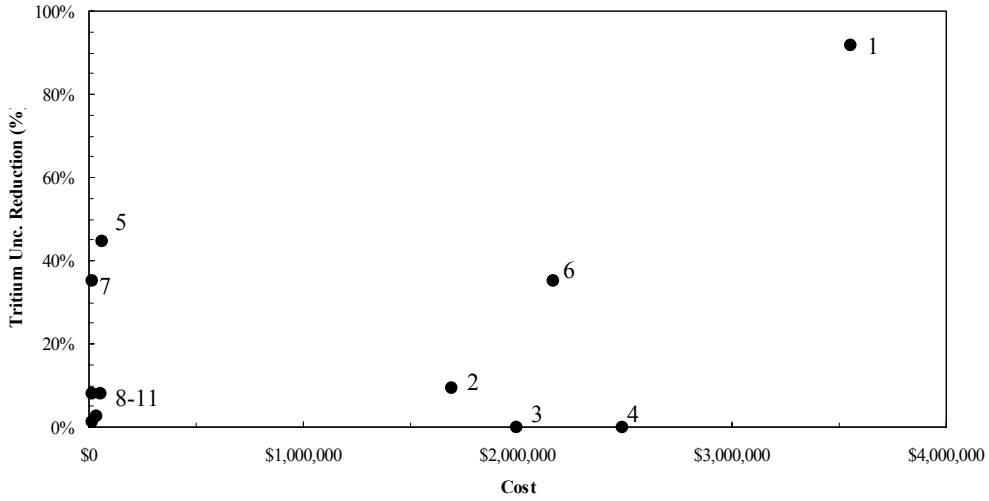

Figure 6. Expected model uncertainty reduction (tritium) versus cost for potential field activities.

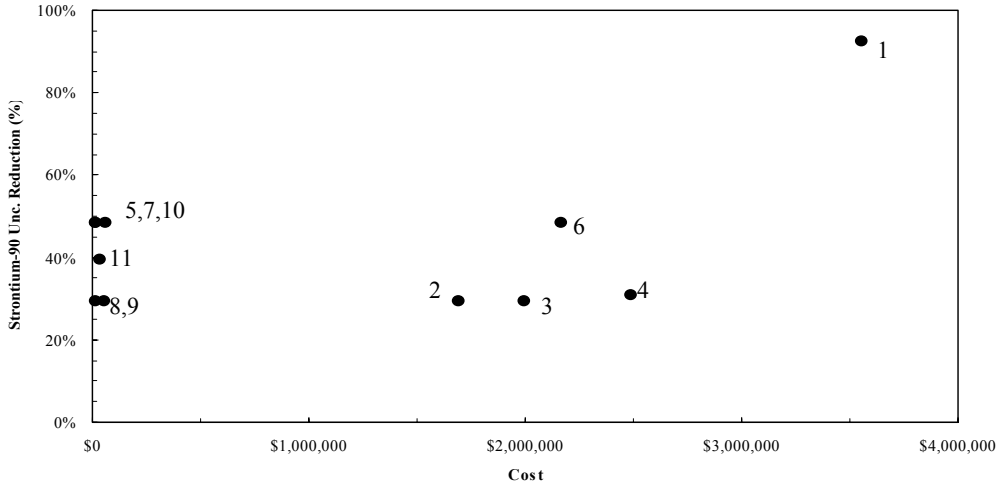

Figure 7. Expected model uncertainty reduction (strontium-90) versus cost for potential field activities.

VI. CONCLUSIONS

A three-dimensional numerical groundwater flow and transport model was developed to estimate radionuclide migration from the CNTA. The model indicated limited transport, but large uncertainties were recognized in a number of important parameters. A quantitative analysis of the uncertainty was performed in a process known as a Data Decision Analysis (DDA). The goal of the DDA was to provide decision makers with the ability to make informed decisions regarding the best course toward site closure.

The DDA identified six uncertain parameters including the specified head boundaries, the spatial distribution of the underlying welded tuff, effective porosity, sorption coefficients, matrix diffusion coefficient, and geochemical release function for the nuclear glass dissolution. Combining the uncertainty in these parameters listed above propagates to a prediction uncertainty in the maximum radius of the contaminant boundary of 234 to 308 m and 234 to 302 m, for tritium and strontium-90, respectively. Although the uncertainty in the input parameters is large, the prediction uncertainty in the contaminant boundary is relatively small, with the range of the 90 percent confidence bounds being 74 and 68 m, for tritium and strontium-90, respectively.

VIII. ACKNOWLEDGEMENTS

The work upon which this paper is based was supported by the U.S. Department of Energy under contract #DE-AC-08-00NV13609. The DOE supervisor is Monica Sanchez, whose continued support and guidance is appreciated. The authors also appreciate the continued support and contributions from Peter Sanders. The contributions of the NDEP supervisor for Shoal, Sigurd Juanarajs, are also acknowledged.

VII. REFERENCES

1. PRUDIC, D.E., J.R. HARRILL and T.J. BURBEY. Conceptual Evaluation of Regional Ground-Water Flow in the Carbonate Rock Province of the Great Basin, Nevada, Utah, and Adjacent States. U.S. Geological Survey, Open-File Report 93-170, 103 p. (1993).

2. U.S. DEPARTMENT OF ENERGY. United States Nuclear Tests, July 1945 through September 1992. Nevada Operations Office Report DOE/NV-209 Rev. 15 (2000).

3. POHLMANN, K., J. CHAPMAN, A. HASSAN and C. PAPELIS. Evaluation of Groundwater Flow and Transport at the Faultless Underground Nuclear Test, Central Nevada Test Area. Desert Research Institute, Division of Hydrologic Sciences, Pub. 45165 (1999).

4. DEUTSCH, C.V. and A.G. JOURNEL. GSLIB Geostatistical Software Library and User's Guide. Second Edition, Oxford University Press (1998).

5. BEVEN, K.J. Prophecy, reality and uncertainty in distributed hydrological modeling. *Advances in Water Resources*, **16**, 41 (1993).

6. CVETKOVIC, V. and G. DAGAN. Transport of kinetically sorbing solute by steady random velocity in heterogenous porous formations. *Journal of Fluid Mechanics*, **265**, 189 (1994).

7. BEVEN, K.J. and A. BINLEY. The future of distributed models: Model calibration and uncertainty prediction. *Hydrologic Processes*, **6**, 270 (1992).